Original Article
ISSN (Online): 2350-0530
ISSN (Print): 2394-3629

International Journal of Research - GRANTHAALAYAH
June 2025 13(6), 11–19

NUMERICAL ANALYSIS OF FLEXURAL STRENGTH AND DUCTILITY OF RU-NC COMPOSITE CIRCULAR COLUMNS

Zhizhou Bai [1], John Chen [2]

[1] Assistant Professor, College of Civil Engineering, Tongji University, Shanghai, China & Honorary Research Associate, Department of Civil Engineering, The University of Hong Kong, Hong Kong, China
[2] Associate, Binnies Hong Kong Limited, Hong Kong, China & Honorary Research Associate, Department of Civil Engineering, The University of Hong Kong, Hong Kong, China

Received 10 April 2025
Accepted 12 May 2025
Published 30 June 2025

Corresponding Author
Zhizhou Bai, zzbai@tongji.edu.cn

DOI
10.29121/granthaalayah.v13.i6.2025.6208

Funding: This research received no specific grant from any funding agency in the public, commercial, or not-for-profit sectors.

ABSTRACT

To theoretically investigate the flexural strength and ductility of a novel composite column structure comprising a Reinforced Ultra-High Performance Concrete (RU) shell and a core Normal Concrete (NC), this study proposes a comprehensive full-range moment-curvature analysis framework. Based on the derived moment-curvature relationships, a comparative analysis is conducted between RU-NC composite circular columns and conventional NC circular columns. The results demonstrate that replacing the NC outer layer with a thin-walled UHPC shell leads to significant enhancements in both flexural strength and ductility performance. Key findings reveal that the flexural strength and ductility of both traditional NC and proposed composite RU-NC circular columns exhibit strong dependence on the applied compressive axial load level. Furthermore, these mechanical properties show a pronounced correlation with the compressive strength of UHPC. Specifically, both flexural strength and ductility are further influenced by the compressive strength of UHPC. As the UHPC compressive strength increases, these mechanical properties exhibit a marked improvement.

Keywords: Ultra-High-Performance Concrete, Full-Range Moment-Curvature Curve, Flexural Strength and Ductility

1. INTRODUCTION

Ultra-high Performance Concrete (UHPC), as an ultra-strong and durable cement-based material, is effectively capable to protect structures from harsh environmental erosion and extend their service life Larrard and Sedran (1994), Richard and Cheyrezy (1995). In comparison to traditional Normal Concrete (NC), UHPC demonstrates superior tensile properties, resulting in significantly improved cracking resistance and enhanced corrosion prevention capabilities.

Many studies on the material properties of UHPC have been performed. Abrishambaf et al. (2017) investigated the effect of steel fiber on the axial tensile properties of UHPC and developed a novel method for calculating the axial tensile strength of UHPC. Shaikh et al. (2020). found that when the water-to-binder ratio (W/B) is below 0.2, the optimal steel fiber content in UHPC ranges from 2% to 3%. Wille et al. (2011) successfully prepared UHPC with good fluidity and excellent performance by using low-heat cement and ultra-fine silica fume without the need for thermal curing.

UHPC is characterized by its significantly reduced porosity and highly compact microstructure, ensuring exceptional resistance to permeability due to its low W/B Abbas et al. (2015). A reduction of one order of magnitude in chloride ion diffusion coefficient is observed in UHPC when contrasted with NC. According to Roux et al. (1996), the chloride ion diffusion coefficients at a testing age of 1 year measured for C30, C80, and UHPC were 1.1 x 10-12, 6.0 x 10-12, and 0.2 x 10-13 m2/s, respectively. The diffusion coefficient has also been found to depend on factors such as W/B, curing conditions, solution concentration, steel fiber volume, and testing age and ranges from 0.2 x 10-13 to 0.41 x 10-12 m^2/s in various studies Kravanja et al. (2024).

In recent years, UHPC has been increasingly applied in the field of bridge engineering. The Sherbrooke Footbridge, erected in Sherbrooke, Canada, in 1997, stands as the world's first engineering marvel to be built using UHPC Blais and Couture (1999). In 2014, China's Hebei Province constructed the nation's first road bridge utilizing prestressed UHPC box girders Chen et al. (2021). The application of UHPC in bridge superstructures has become widespread across the globe now Graybeal et al. (2020).

Several advanced techniques utilizing UHPC have also been proposed for seismic retrofitting of existing columns and have been successfully implemented in a number of real-world applications. Beschi et al. (2011), Doiron (2016). In addition to the application of UHPC in strengthening existing columns, various scholars have also proposed the concept of utilizing UHPC shells during the design phase. This involves using the UHPC shell as both the formwork for the core NC and the permanent load-bearing structure, thereby forming a UHPC-NC composite column Lin et al. (2017).

Lin et al. (2017) proposed a 100 mm thick UHPC shell scheme without reinforcement, while the core NC was reinforced. This composite circular column is referred to as the U-RC composite column in their work. Shan et al. (2021)conducted experimental research on the hysteretic loading performance of U-RC composite circular columns with UHPC shells provided with spiral hoops, discovering that they may exhibit superior seismic performance compared to traditional NC columns.

The use of UHPC shells during the design phase enhances durability of columns in harsh environments and significantly reduces steel formwork requirements, eliminates the need for formwork removal, offering potential cost-saving benefits. Huang et al. (2022) proposed an improved scheme to translate the reinforcement cage from the core concrete to UHPC and is referred to as the RU-NC composite column. In contrast to the U-RC composite columns, the RU-NC column features a reinforced UHPC shell, while its core NC remains unreinforced. The experimental study on RU-NC composite circular columns indicates that it may even enhance the axial compression performance.

When reinforcing UHPC shells, the combination of steel reinforcement and UHPC can create a complementary effect, theoretically enhancing bending, compression, and shear resistance, as well as further improving crack resistance,

thereby offering greater advantages. Meanwhile, the circular shape is a very commonly used cross-sectional form for piers and columns. In response to this, this study develops a full-range moment-curvature analysis method for RU-NC composite columns. And the method was applied to analyze and assess the flexural strength and ductility of RU-NC composite circular columns. The results are compared with those of traditional NC circular columns, yielding some beneficial conclusions that can serve as a reference for related research and application for RU-NC composite circular columns.

2. CONSTITUTIVE MODELS OF MATERIALS

2.1. NC

The compressive behavior of NC follows the constitutive model by Attard and Setunge (1996). This model requires four primary parameters: (a) peak stress fco, (b) its associated strain εco, and (c) two shape coefficients A and B. The model is expressed as

$$\frac{\sigma_c}{f_{co}} = \frac{Ax+Bx^2}{1+(A-2)x+(B+1)x^2}\ , x = \frac{\varepsilon_c}{\varepsilon_{co}} \tag{1}$$

The parameters A and B are determined by

$$\begin{cases} A = \frac{E_c\varepsilon_{co}}{f_{co}}, B = \frac{(A-1)^2}{0.55} - 1 & x \le 1 \\ A = \frac{f_{ci}(\varepsilon_{ci}-\varepsilon_{co})^2}{\varepsilon_{co}\varepsilon_{ci}(f_{co}-f_{ci})}, B = 0 & x > 1 \end{cases} \tag{2}$$

The parameters E_c, ε_{co}, f_{ci} and ε_{ci} are determined as

$$E_c = 4370(f_{co})^{0.52} \tag{3a}$$

$$\varepsilon_{co} = 4.11(f_{co})^{0.75}/E_c \tag{3b}$$

$$\frac{f_{ci}}{f_{co}} = 1.41 - 0.17\,ln(f_{co}) \tag{3c}$$

$$\frac{\varepsilon_{ci}}{\varepsilon_{co}} = 2.50 - 0.30\,ln(f_{co}) \tag{3d}$$

2.2. UHPC

The compressive behavior of UHPC follows the constitutive model by Yang and Fang (2009), where the stress σ_c is expressed as a function of normalized strain $x = \frac{\varepsilon_c}{\varepsilon_{co}}$. This model requires three key inputs: (a) peak stress fco, (b) its associated strain εco, and (c) shape coefficient A. The model is expressed as

$$\frac{\sigma_{co}}{f_{co}} = \begin{cases} \frac{Ax-x^2}{1+(A-2)x} & x \le 1 \\ \frac{x}{2(x-1)^2+x} & x > 1 \end{cases} \tag{4}$$

The parameters A, E_c (in MPa) and ε_{co} are determined as

$$A = \frac{E_c \varepsilon_{co}}{f_{co}} \tag{5a}$$

$$E_c = \frac{10^3}{0.0172 + 0.8364 f_{co}} \tag{5b}$$

$$\varepsilon_{co} = (6.7264 f_{co} + 2460.9) 10^{-6} \tag{5c}$$

Figure 1 shows one typical stress–strain curve of NC with fco = 30MPa, along with three typical stress–strain curves of UHPC with fco = 100, 120 and 140MPa respectively used in this study.

Figure 1

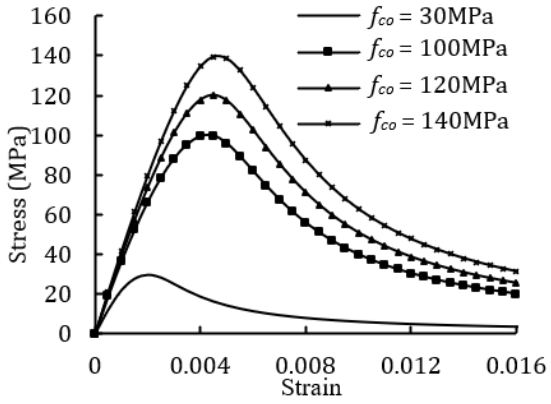

Figure 1 Typical Stress–Strain Curves of NC and UHPC

2.3. STEEL REINFORCEMENT

An idealized bilinear stress-strain model is applied to the steel reinforcement, where the stress σ_s relates to the strain ε_s as

$$\begin{cases} \sigma_s = E_s \varepsilon_s & \varepsilon_s \le f_y / E_s \\ \sigma_s = f_y & \varepsilon_s > f_y / E_s \end{cases} \tag{6}$$

where E_s characterizes the elastic stiffness and f_y defines the yield plateau onset.

3. METHODS OF ANALYSIS

The analytical model begins with the application of a concentric axial load P (compression positive) prior to flexural loading. Consistent with conventional RC design practice and those findings by Bai and Au (2009), the tensile contributions of both NC and UHPC are excluded. The plane-section hypothesis enforces strain compatibility between steel and adjacent concrete. As can be seen in Figure 2, for a cross-section subjected to curvature ϕ, the longitudinal strain ε at

coordinate x relates to the neutral axis position d_n through the kinematic relationship as

$$\varepsilon = \varphi(d_n - x) \tag{7}$$

Based on the established constitutive laws of the materials, the stress distributions in both concrete and steel reinforcement can be quantitatively determined. These internal stresses developed in the cross-section must collectively satisfy the fundamental equilibrium conditions, ensuring that their resultant forces equilibrate the external axial load and flexural moment about the geometric centroid.

To establish the moment-curvature response of a section, the neutral axis position must first be solved iteratively under deformation compatibility. For a prescribed curvature ϕ, an initial estimate of the neutral axis depth dn is typically non-equilibrium, leading to an unbalanced longitudinal force. Due to the nonlinear coupling between dn and sectional forces, numerical iteration becomes essential to achieve force equilibrium. By progressively increasing ϕ from zero until the moment capacity degrades substantially, the full-range moment-curvature relationship, including strain-softening regimes, can be traced.

Figure 2

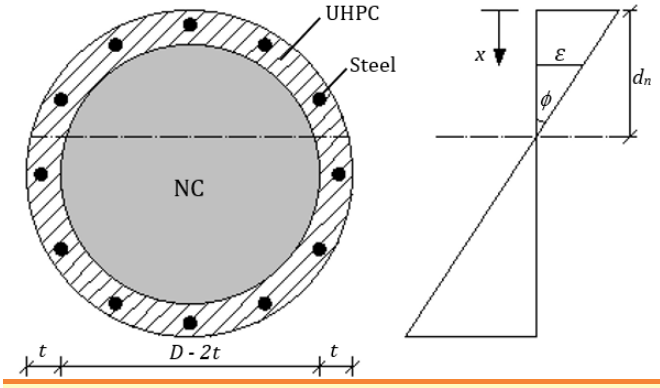

Figure 2 An RU-NC Composite Circular Column Section

4. OUTCOMES OF NUMERICAL ANALYSIS

4.1. CIRCULAR SECTIONS

The circular sections analysed are with a typical diameter D = 1000 mm, with a UHPC shell thickness t = 100 mm. The steel reinforcement, with a cover c = 50 mm, has and elastic modulus Es = 200GPa and yields at fy = 400 MPa. The fnc, namely the in situ compressive strength of NC, is set at 30MPa, while fuc, namely that of UHPC, is considered for three cases: 100 MPa, 120 MPa and 140 MPa. Bai (2006) investigated size effects through a proposed normalization approach employing dimensionless parameters, enabling the extension of findings to geometrically scaled models with shared material and reinforcement properties. The current study specifically excludes discussion of confinement mechanisms. The reinforcement ratio $\rho_s = \frac{A_s}{\pi D^2}$, in which $A_s$is the total area of steel reinforcement, is considered for two cases: 1% and 2%. It is assumed that the steel reinforcement is uniformly and densely arranged along the same circumferential radius. The axial

load ratio is defined as P/fncAg, in which P is the resultant axial force and Ag is the gross cross-sectional area of the composite section.

4.2. FULL-RANGE MOMENT-CURVATURE CURVES

As shown in Figure 3 with reinforcement ratio $\rho_s = 1\%$, the typical full-range moment-curvature response of RU-NC circular columns varies significantly with axial load levels. Under low axial load ratios, the post-peak stage exhibits a prolonged plateau, whereas higher axial loads lead to sharper peaks and reduced ductility. The axial force ratio predominantly influences the overall shape of the curves for both NC and RU-NC sections.

On the other hand, for a given axial force ratio, Figure 3 demonstrates the effect of replacing NC by UHPC on the full-range moment curvature response. It can be seen that UHPC not only helps to enhance peak resisting moment but also improve ductility, which is related with fnc. Both flexural strength and ductility increase with fnc increases.

Figure 3

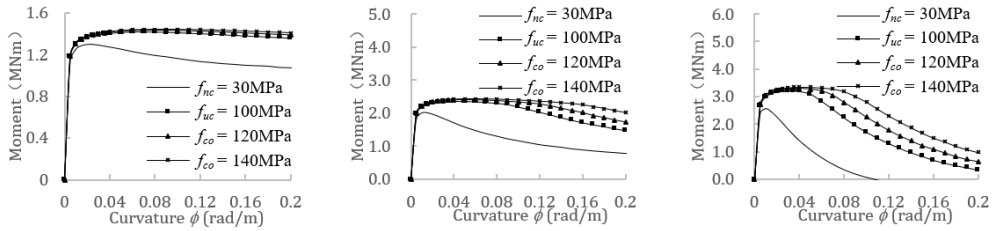

(a) $P/f_{nc}A_g$ = 0.0 (b) $P/f_{nc}A_g$ = 0.1 (c) $P/f_{nc}A_g$ = 0.2

Figure 3 Typical Full-Range Moment-Curvature Curves with $\boldsymbol{\rho_s}$=1%

4.3. FLEXUAL STRENGTH AND DUCTILITY

Figure 4 illustrates the correlation between flexural strength Mr and axial load ratio P/fncAg. It can be seen that the flexural strength Mr tends to increase with the compressive axial load. Obviously, the axial load ratio is an important parameter that determines not only the shape of moment-curvature curve but also the flexural strength. On the other hand, for a given axial force ratio, Figure 4 also demonstrates the effect of replacing NC by UHPC on the flexural strength.

It is clear that the flexural strength increases significantly when UHPC is adopted. The flexural strength ratio of an RU-NC circular column section to an NC circular column section for fuc 100MPa, 120 MPa and 140 MPa, respectively, is 1.099, 1.185 and 1.289 with axial load ratio P/fncAg = 0.1 and $\rho_s = 1\%$. Slightly higher flexural strength ratios can be obtained when the axial load ratio P/fncAg or the reinforcement ratio ρ_s increases.

Figure 4

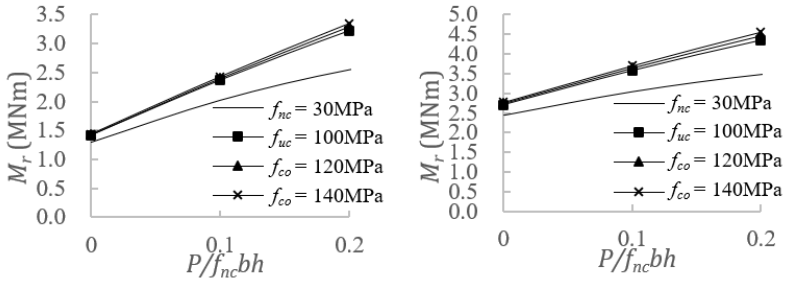

(a) $\rho_s = 1\%$ (b) $\rho_s = 2\%$

Figure 4 Flexural Strength of RU-NC Circular Columns

The flexural ductility factor μ can be evaluated using ultimate curvature ϕ_u and yield curvature ϕ_y based on the full-range moment-curvature curve as

$$\mu = \phi_u / \phi_y \tag{8}$$

The ultimate curvature ϕ_u is the section curvature corresponding to a resisting moment decayed to 85% of the peak moment. The yield curvature ϕ_y is defined as the curvature at the idealized yield point of an equivalent elastic-perfectly plastic system, where the elastic stiffness matches the secant stiffness at 75% of the peak moment, and the yield moment equals the peak moment.

As shown in Figure 5, the correlation between flexural ductility μ and axial load ratio P/fncAg is presented. It can be seen that when the compressive axial load increases, the flexural ductility μ generally reduces. Figure 5 also demonstrates the effect of replacing NC by UHPC. Notably, the use of UHPC significantly enhances flexural ductility.

The flexural ductility ratio of an RU-NC circular section to an NC circular section for fuc 100MPa, 120 MPa and 140 MPa, respectively, is 2.736, 3.454 and 4.243 with axial load ratio P/fncAg = 0.1 and $\rho_s = 1\%$. While that with axial load ratio P/fncAg = 0.2 and $\rho_s = 1\%$, respectively, is 2.337, 2.916 and 3.532. The flexural ductility ratio is relatively sensitive and decreases with axial load ratio P/fncAg. Such value with axial load ratio P/fncAg = 0.1 and $\rho_s = 2\%$, respectively, is 2.001, 2.406 and 2.839. It seems that the flexural ductility ratio is also relatively sensitive and decreases with reinforcement ratio ρ_s.

Figure 5

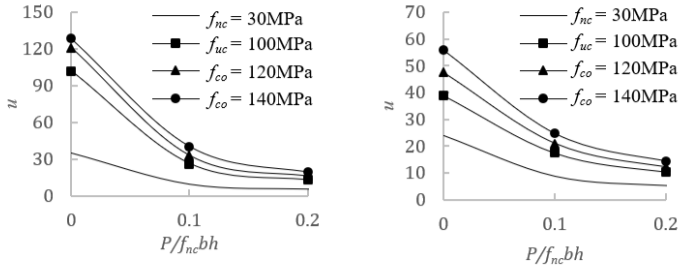

(a) $\rho_s = 1\%$ (b) $\rho_s = 2\%$

Figure 5 Flexural Ductility of RU-NC Circular Columns

5. CONCLUSION

Due to its exceptional performance, UHPC has witnessed increasingly widespread applications in recent years. UHPC is relatively expensive in material cost, resulting in significantly higher construction expenses for pure UHPC structures. Consequently, developing UHPC composite structures has emerged as a viable alternative solution.

This study investigates a novel UHPC composite circular column structure featuring reinforced UHPC thin-walled shells encasing NC cores, which is designed to achieve long service life in harsh environments. To evaluate the flexural performance of this innovative RU-NC composite circular column, a comprehensive full-range moment-curvature analysis procedure was developed and implemented for theoretical investigation.

Key findings demonstrate that the proposed RU-NC configuration not only enhances structural strength directly but also significantly improves ductility performance. These results substantiate the system's guaranteed seismic resistance capacity, suggesting its effectiveness for earthquake-resistance.

CONFLICT OF INTERESTS

None.

ACKNOWLEDGMENTS

The work carried out herein is supported by National Natural Science Foundation of China (NSFC 52178297).

REFERENCES

Abbas, S., Soliman, A. M., & Nehdi, M. L. (2015). Exploring Mechanical and Durability Properties of Ultra-High Performance Concrete Incorporating Various Steel Fiber Lengths and Dosages. Construction and Building Materials, 75, 429–441. https://doi.org/10.1016/j.conbuildmat.2014.11.017

Abrishambaf, A., Pimentel, M., & Nunes, S. (2017). Influence of Fibre Orientation on the Tensile Behaviour of Ultra-High Performance Fibre Reinforced Cementitious Composites. Cement and Concrete Research, 97, 28–40. https://doi.org/10.1016/j.cemconres.2017.03.007

Attard, M. M., & Setunge, S. (1996). Stress-Strain Relationship of Confined and Unconfined Concrete. ACI Materials Journal, 93(5), 432–442. https://doi.org/10.14359/9847

Bai, Z. Z. (2006). Nonlinear Analysis of Reinforced Concrete Beams and Columns with Special Reference to Full-Range and Cyclic Behaviour [Doctoral Dissertation, The University of Hong Kong]. Proquest Dissertations & Theses Global.

Bai, Z. Z., & Au, F. T. K. (2009). Ductility of Symmetrically Reinforced Concrete Columns. Magazine of Concrete Research, 61(5), 345–357. https://doi.org/10.1680/macr.2008.00149

Beschi, C., Meda, A., & Riva, P. (2011). Column and Joint Retrofitting with High Performance Fiber Reinforced Concrete Jacketing. Journal of Earthquake Engineering, 15(7), 989–1014. https://doi.org/10.1080/13632469.2011.552167

Blais, P. Y., & Couture, M. (1999). Precast, Prestressed Pedestrian Bridge—World's First Reactive Powder Concrete Bridge. PCI Journal, 44(5), 60–71. https://doi.org/10.15554/pcij.09011999.60.71

Chen, B. C., Huang, Q. W., Su, J. Z., Guo, B., & Ma, X. L. (2021). Design and Construction of the First UHPC Highway Box-Girder Bridge in China. Journal of China and Foreign Highway, 41(5), 74–78. https://doi.org/10.14048/j.issn.1671-2579.2021.05.016

Doiron, G. (2016). Pier Repair/Retrofit Using UHPC: Examples of Completed Projects in North America. International Interactive Symposium on Ultra-High Performance Concrete, 1(1). https://doi.org/10.21838/uhpc.2016.99

Graybeal, B., Brühwiler, E., & Kim, B. S. (2020). International Perspective on UHPC in Bridge Engineering. Journal of Bridge Engineering, 25(11), 04020094. https://doi.org/10.1061/(ASCE)BE.1943-5592.0001630

Huang, Q. W., Wang, S. R., Huang, W., Chen, B. C., Wei, J. G., & Chen, Q. Y. (2022). Mechanical Behavior of RU-NC Composite Short Columns Under Axial Compressive Loads. Journal of Hunan University (Natural Sciences), 49(11), 137–149. https://doi.org/10.16339/j.cnki.hdxbzkb.2022124

Kravanja, G., Mumtaz, A. R., & Kravanja, S. (2024). A Comprehensive Review of the Advances, Manufacturing, Properties, Innovations, Environmental Impact and Applications of Ultra-High-Performance Concrete (UHPC). Buildings, 14(2), 382. https://doi.org/10.3390/buildings14020382

Larrard, F. D., & Sedran, T. (1994). Optimization of Ultra-High-Performance Concrete by the use of a Packing Model. Cement and Concrete Research, 24(6), 997–1009. https://doi.org/10.1016/0008-8846(94)90022-1

Lin, S. S., Huang, Q. W., Chen, B. C., & Chen, Y. H. (2017). Design of U-RC Composite Pier of Sea-Crossing Bridge. Journal of Traffic and Transportation Engineering, 17(4), 55–65.

Richard, P., & Cheyrezy, M. (1995). Composition of Reactive Powder Concretes. Cement and Concrete Research, 25(7), 1501–1511. https://doi.org/10.1016/0008-8846(95)00144-2

Roux, N., Andrade, C., & Sanjuan, M. A. (1996). Experimental Study of Durability of Reactive Powder Concretes. Journal of Materials in Civil Engineering, 8(1), 1–6. https://doi.org/10.1061/(ASCE)0899-1561(1996)8:1(1)

Shaikh, F. U. A., Luhar, S., Arel, H. S., & Luhar, I. (2020). Performance Evaluation of Ultrahigh Performance Fibre Reinforced Concrete—A Review. Construction and Building Materials, 232, 117152. https://doi.org/10.1016/j.conbuildmat.2019.117152

Shan, B., Liu, G., Li, T. Y., Liu, F. C., Liu, Z., & Xiao, Y. (2021). Experimental Research on Seismic Behavior of Concrete-Filled Reactive Powder Concrete Tubular Columns. Engineering Structures, 233, 111921. https://doi.org/10.1016/j.engstruct.2021.111921

Wille, K., Naaman, A. E., & Parra-Montesinos, G. J. (2011). Ultra-High Performance Concrete with Compressive Strength Exceeding 150 MPa (22 ksi): A Simpler Way. ACI Materials Journal, 108(1), 34–36. https://doi.org/10.14359/51664215

Yang, J., & Fang, Z. (2009). Flexural Behaviors of Ultra-High Performance Concrete T Beams Prestressed with CFRP Tendons. Journal of the China Railway Society, 31(2), 94–103. https://doi.org/10.3969/j.issn.1001-8360.2009.02.018